NRC Research Press

ARTICLE

Sintered polymeric binders for Li-ion battery alloy anodes

T.D. Hatchard, R.A. Fielden, and M.N. Obrovac

Abstract: The cycling performance in lithium half cells of Si alloy electrodes with polyvinylidene fluoride or polyimide binders were evaluated after the electrodes were cured at temperatures below and above the binder carbonization temperature. After carbonization, the cycling performance of electrodes using polyvinylidene fluoride binder improved considerably but still suffered from capacity fade. Electrodes with carbonized polyimide binder had superior performance and showed no capacity fade after 100 cycles. The superior performance of carbonized polyimide electrodes is thought to be related to polyimide's high carbon yield upon heating, resulting in the formation of a uniform carbon coating on alloy surfaces. These results suggest that new high performance binders for alloy electrodes might be derived by the carbonization of polymers with a high carbon yield that lead to the formation of uniform carbon coatings on alloy particles.

Key words: lithium-ion batteries, alloy negative electrodes, silicon alloys, electrode binders.

Résumé : Nous avons évalué la performance de cycle de demi-cellules Li constituées d'électrodes en alliage de Si à liants de fluorure de polyvinylidène ou de polyimide, après cuisson des électrodes à des températures inférieures et supérieures à la température de carbonisation du liant. Après carbonisation, bien que la performance de cycle des électrodes à liant de fluorure de polyvinylidène ait été considérablement améliorée, elle accusait toujours une perte de capacité. Les électrodes à liant de polyimide carbonisé présentaient pour leur part une meilleure performance, et ce, sans aucune perte de capacité après 100 cycles. Nous pensons que la performance supérieure des électrodes à liant de polyimide carbonisé serait liée au rendement en carbone élevé du polyimide lors du chauffage, ce qui permet de former une couche de carbone uniforme à la surface des alliages. Ces résultats laissent supposer que de la carbonisation de polymères à haut rendement en carbone pourrait permettre d'en dériver de nouveaux liants à haute performance destinés aux électrodes en alliage, grâce à la formation d'une couche de carbone uniforme sur les particules d'alliage. [Traduit par la Rédaction]

Mots-clés : batteries au lithium-ion, électrodes négatives en alliage, alliages de silicium, liants d'électrode.

Introduction

A promising avenue to achieve the goals of lower cost and higher energy density in lithium-ion (Li-ion) cells is the use of alloy anodes based on abundant materials such as Si or Sn. Si and Sn alloys can result in high energy density gains when implemented in Li-ion cells.[1] The drawback of these materials is their large volume expansion upon lithiation, which is 280% for pure Si.[1–3] This volume expansion causes cracking and pulverization of the electrode and disruption of the solid electrolyte interphase (SEI), which leads to capacity loss and failure of the cell. It also can result in mechanical failure of the electrode, requiring the use of special polymer binders.[1]

It has been found that binders that perform well in alloy coatings have certain specific properties. These are as follows: good adhesion to both the alloy particles and the current collector, complete surface coverage of the alloy particles to reduce electrolyte decomposition, and the ability to tolerate volume expansion by stretching or self-healing to maintain the structural integrity of composite coatings.[1,4–11] It has been suggested that good surface coverage of the binder is required to form an "artificial SEI layer", which minimizes further SEI formation, thus reducing irreversible capacity.[8] It has also been shown that electrically conducting polymer binders that fully encapsulate the alloy particles not only provide the benefits described, but also form a conductive matrix that leads to improved cycling by maintaining particle electrical contact.[12,13] Recently, we have suggested that electroactive binders such as polyimide or phenolic resin undergo full reduction to hydrogen-containing carbons when lithiated to 0 V.[9,10] The resulting electrode, now an alloy–carbon composite with no polymer binder, has excellent cycling performance. Apparently, the hydrogen-containing carbon serves as a conductive binder and, in addition, provides additional capacity to the electrode. This effect has been recently confirmed by Yoon et al.[14] We suspect that most conductive binders that have been proposed are reduced during lithiation and work in a similar manner.

Because binders that undergo electrochemical reduction to carbon perform well, this naturally begs the question as to whether a thermally carbonized binder would perform equally well. Carbonized binders have been used for structural materials, e.g., in carbon–carbon composites. Hassan et al. have reported the use of sintered PVDF as an effective binder for a Si nanoparticle electrode.[15] In this study, the use of carbonized polymers as high performance binders in alloy electrodes will be explored using carbonized aliphatic PVDF and aromatic polyimide (PI) binders.

Received 28 November 2017. Accepted 29 January 2018.

T.D. Hatchard and R.A. Fielden. Department of Chemistry, Dalhousie University, Halifax, NS B3H 4R2, Canada.
M.N. Obrovac. Department of Chemistry, Dalhousie University, Halifax, NS B3H 4R2, Canada; Department of Physics and Atmospheric Science, Dalhousie University, Halifax, NS B3H 4R2, Canada.
Corresponding author: M.N. Obrovac (email: mnobrovac@dal.ca).

This paper is part of a Special Issue to celebrate the 200th anniversary of Dalhousie University in Halifax, Nova Scotia, Canada.

Experimental

Electrode preparation

Electrode coatings were made by mixing 3M L-20772 V6 Si alloy (hereafter called V6; 3 μm, from 3M Co., St. Paul, MN) and graphite (SFG6L Timcal), as well as binder and carbon black (C-NERGY Super C 65, Timcal), in N-methyl-2-pyrrolidone (NMP, Sigma Aldrich, anhydrous 99.5%) in a 60/28/2/10 V6/SFG6L/SuperC/binder weight ratio. Binders used were polyvinylidene fluoride resin (PVDF, HSV 900 Kynar®) and aromatic polyimide (PI, purchased as a 20% solution of polyamic acid in NMP, HD MicroSystems). One PVDF electrode was formulated to have double the amount of binder, resulting in a 60/28/2/20 V6/SFG6L/SuperC/binder weight ratio. Electrode slurries were mixed for 1 h in a Retsch PM200 planetary mill at 100 rpm with four 0.5 inch (1 inch = 2.54 cm) tungsten carbide balls and then spread onto copper or nickel foil with a 0.004 inch doctor blade. Coatings were dried in air at 120 °C for 1 h. After drying in air, circular disks with an area of 1.9 cm^2 were punched from the electrode coatings to be used as cathodes in Li half cells. These disks were then heated to 600 °C at a rate of 10 °C min^{-1} in flowing Ar and held for 3 h. Exhaust gas from the tube furnace was flowed through an oil bubbler and then through a water bubbler containing calcium carbonate chips to neutralize any HF produced during the annealing of films containing PVDF. After cooling, the disks were transferred to an Ar-filled glove box without air exposure. Alloy-containing electrodes are designated here with the notation alloy/graphite/binder(heating temperature), e.g., alloy/graphite/PVDF(600 °C). The specific capacities of these alloy-containing electrodes are reported here in terms of the total electrode coating mass.

Binder only electrodes were made by spreading 20% (wt) slurries of PVDF or PI in NMP on Cu foil with a 0.004 inch doctor blade. Coatings were dried in air at 120 °C for 1 h. After drying in air, circular disks with an area of 1.9 cm^2 were punched from the electrode coatings to be used as cathodes in Li half cells. Some of these disks were then heated to 300 °C or 600 °C at a rate of 10 °C min^{-1} in flowing Ar and held for 3 h. Tube furnace exhaust was treated as described above. TiN/PI electrodes were prepared with an 83/17 v/v ratio by the same method as described in Wilkes et al.[9] The specific capacities of such electrodes are reported here in terms of the mass of binder as measured after heating at 120 °C.

Electrode structural analysis

X-ray diffraction (XRD) patterns of unheated and heated binder powders were collected with a Rigaku Ultima IV diffractometer equipped with a diffracted beam graphite monochromator, scintillation detector, and a Cu Kα radiation source. Polyamic acid powder was obtained by heating a 20% solution of polyamic acid in NMP (HD Microsystems) in air at 120 °C overnight and grinding the resulting solid residue. The resulting powder was heated in flowing argon for 3 h at 300 °C or 600 °C. Heated PVDF powder was obtained by heating PVDF as received under flowing argon for 3 h at 600 °C. Scanning electron microscopy (SEM) was performed using a Hitachi S-4700 Field Emission SEM.

Coin cell preparation

The disks that were previously cut from the electrode coatings and heated under Ar, as described above, were used as working electrodes in Li half cells. Typical active material loadings were about 1.8–2.0 mAh cm^{-2} for V6/graphite electrodes. Coin cells were assembled in an Ar-filled glove box. Lithium metal foil was used as the counter electrode. Two layers of Celgard 2301 were used as separators. Then, 1 mol L^{-1} $LiPF_6$ in a solution of ethylene carbonate, diethyl carbonate, and monofluoroethylene carbonate (1 mol L^{-1} $LiPF_6$ in EC/DEC/FEC; 3:6:1 by volume, BASF) were used as the electrolyte. Coin cells were cycled using a Maccor Series 4000 Automated Cycler. V6/graphite electrodes were cycled with potential limits of 0.005–1.5 V for the first cycle with a rate of C/10 and a C/40 trickle discharge at 0.005 V. Subsequent cycling was performed between 0.005 and 0.900 V at a rate of C/4 with a C/20 trickle discharge at 0.005 V. Binder only and binder/TiN electrodes were cycled between limits of 0.005 and 2.0 V at a rate of C/25 with a C/50 trickle discharge at 0.005 V.

Fig. 1. TGA curves of polyamic acid and PVDF collected at a heating rate of 5 °C min^{-1} under Ar gas. [Colour online.]

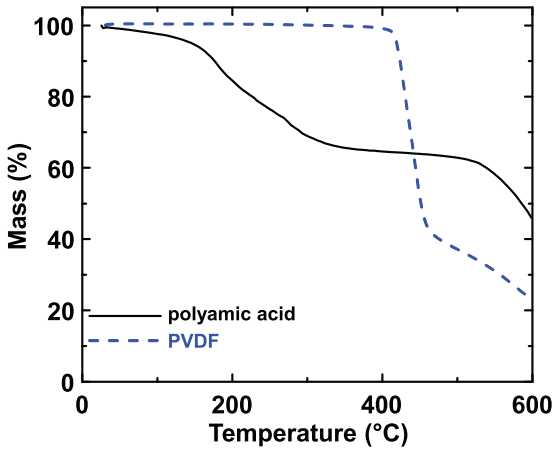

Thermogravimetric analysis

Thermogravimetric analysis (TGA) was performed using a TG 209 F3 (Netzsch) in Ar. Samples of the dried binders were placed in Al_2O_3 cups and then loaded into the heating chamber. The chamber was purged with Ar to remove any air before heating. Heating rate was 5 °C min^{-1} to a maximum temperature of 600 °C.

Results

Figure 1 shows the TGA curves of polyamic acid and PVDF. PVDF is stable at temperatures up to about 420 °C. Above 400 °C, PVDF decomposes, resulting in a rapid mass loss, with only about 20% of the initial mass remaining at 600 °C. This behavior is typical of aliphatic polymers and results in the formation of hydrogen containing carbons as a residue,[16] as confirmed by XRD below. The TGA curve for polyamic acid shows that it undergoes an initial rapid mass loss at about 150–300 °C, which is the nominal temperature at which polyamic acid imidizes to form PI. This weight loss can be attributed to the evaporation of water, which is a product of the imidization reaction. The PI formed is then stable to just over 500 °C. Above this temperature, a second rapid mass loss begins that is ongoing at the 600 °C end point of the experiment, corresponding to the thermal carbonization of PI.

Figures 2*a*–2*d* show XRD patterns of PVDF and PI binders heated at the same temperatures used to make the electrode coatings in this study. The XRD pattern of PVDF at 120 °C (Fig. 2*a*) is indicative of crystalline ordering of the polymer. After heating to 600 °C (Fig. 2*b*), the XRD pattern is consistent with a hard carbon with single layer stacking, as has been observed previously.[16] The XRD pattern of PI at 300 °C (Fig. 2*c*) is typical of a disordered polymer with some short range ordering. After heating to 600 °C, the XRD pattern (Fig. 2*d*) is also typical of a hard carbon with single layer stacking.[16]

To directly measure the electrochemistry of cured and sintered PI and PVDF in a composite electrode, electrode coatings were made with these binders and inactive TiN powder, which was used as an inactive conductive filler to take the place of active material. As described in Wilkes et al.,[9] this allows binders to be studied in the same environment as they exist in composite electrode coatings without electrochemical interference from active materials. Figure 3 shows the potential vs. capacity curve of PI and PVDF binders in these electrodes. All capacities are calculated with re-

Fig. 2. XRD patterns of pure binder polymers heated to temperatures as indicated. A Lorentz polarization correction has been applied to the XRD patterns of PVDF and PI heated to 600 °C in (*b*) and (*d*) so that the carbon 002 peak can be plotted more accurately.

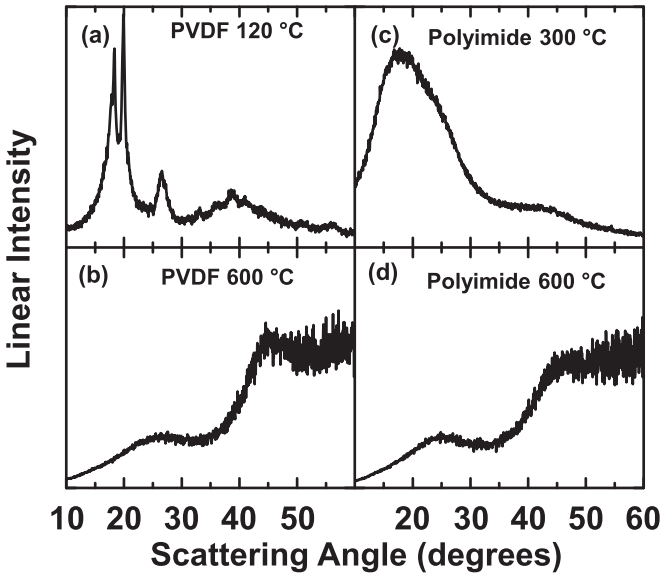

Fig. 3. Potential vs. capacity curves of PVDF and PI binders in TiN/binder coatings after heating to different temperatures, as indicated. Solid and dashed lines are for coatings on Cu and Ni current collectors, respectively.

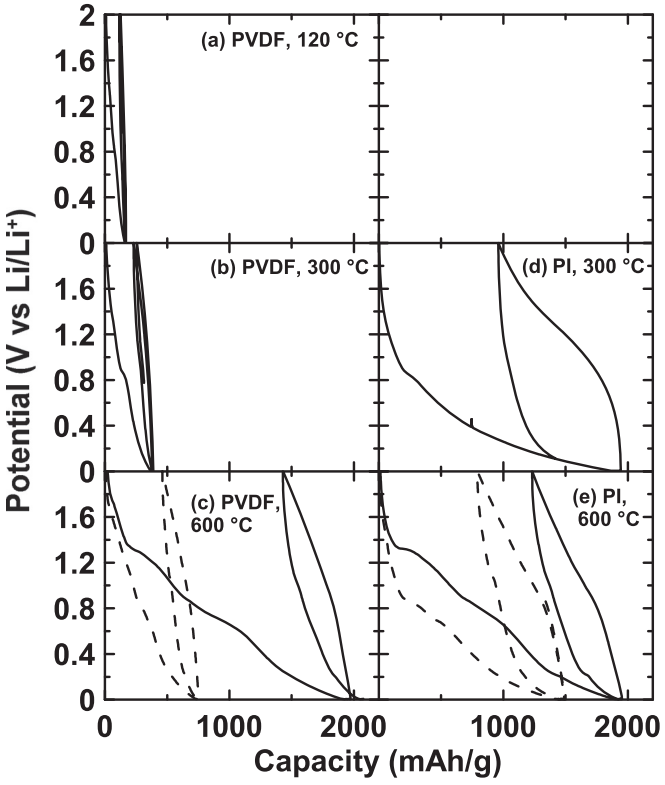

spect to the mass of the binder initially used to prepare the electrodes and are not corrected for the weight loss that occurs during heating. This was done to compare irreversible capacities in a meaningful way. In addition, cell makers would typically measure capacities as a function of the amount of materials added during electrode preparation.

Figures 3*a*–3*c* show the potential vs. capacity curves of TiN/PVDF electrodes after heating to 120 °C, 300 °C, and 600 °C, respectively. PVDF is essentially electrochemically inactive at 120 °C and 300 °C. However, the irreversible capacity at 300 °C is increased. At 600 °C, the TiN/PVDF electrode has considerable irreversible and reversible capacity. We suspect that the increase in irreversible capacity with increasing temperature is related to the formation of Cu_2O on the surface of the current collector foil, despite efforts of maintaining an inert atmosphere. Indeed, the first lithiation potential vs. capacity curve is very similar to that reported for Cu_2O by Grugeon et al., in which Cu_2O is first reduced in a plateau extending from about 1.2 V to 1.5 V followed by a lower potential plateau at about 0.8 V, which was ascribed to capacity from SEI formation.[17] To provide further evidence that this increase in capacity is related to the current collector, the Cu foil current collector of the TiN/PVDF electrode was replaced by Ni foil (also shown in Fig. 3*c*), which is less susceptible to oxidation. This results in the disappearance of the high potential plateau and the irreversible capacity is much reduced. Therefore, we ascribe much of the first discharge capacity of the PVDF electrode that was heated at 600 °C to the oxidation of the Cu current collector. The increased capacity shown in the Ni current collector is likely related to the residual carbon from the decomposition of PVDF.

Figures 3*d* and 3*e* show potential vs. capacity curves of TiN/PI electrodes that were heated at 300 °C and 600 °C, respectively. The potential vs. capacity curve of PI cured at 300 °C has large irreversible capacity, large reversible capacity, and large hysteresis; all of which are typical of hydrogen-containing carbons.[18] We have suggested that PI carbonizes during lithiation previously[9] and this mechanism has been verified by Yoon et al.[14] After heating to 600 °C, the reversible capacity and polarization becomes reduced and the potential vs. capacity curve is similar to that of heated PVDF, shown in Fig. 3*c*. This is consistent with hydrogen loss, which occurs when hydrogen-containing carbons are heated.[18] The plateaus during the first discharge of the TiN/PI electrodes that were heated to 600 °C also resemble those of the TiN/PVDF electrode heated to the same temperature, which we attributed to the formation of Cu_2O. Also shown in Fig. 3*e* is a potential vs. capacity curve of the TiN/PI electrode coated on a Ni current collector and heated to 600 °C. The high potential plateau related to Cu_2O reduction disappears when a Ni current collector is used, but the first cycle capacity below 1 V remains high. This may be due to higher hydrogen content in this aromatic carbon than PVDF heated to the same temperature.

Figures 4*a*–4*d* show SEM images of alloy/graphite/PVDF(120 °C), alloy/graphite/PVDF(600 °C), alloy/graphite/PI(300 °C), and alloy/graphite/PI(600 °C) electrodes, respectively. The PVDF binder is clearly visible in the alloy/graphite/PVDF(120 °C) electrode (Fig. 4*a*) as filaments bridging particles. At 600 °C (Fig. 4*b*), the PVDF is no longer visible. All alloy and graphite surfaces appear smooth and pristine. This is consistent with the TGA results, showing that nearly all of the PVDF decomposes to form gaseous components at this temperature. In contrast, alloy particles in the alloy/graphite/PI(300 °C) electrode (Fig. 4*c*) are all covered with a rough, granular layer of PI polymer. Despite the surface roughness, all alloy particles were found to be completely coated with this PI layer, whereas the graphite particles appear pristine. PI binder's ability to form a uniform coating on the alloy particles is likely due to the strong ester-like bonds formed between PI and Si alloys.[9] These are due to the reaction of carboxylic acid groups of poly(amic acid) with silanol groups (Si–OH) on the surface of silicon alloys. At 600 °C (Fig. 4*d*), there is little change. All graphite particle surfaces appear pristine, whereas a rough, but uniform, coating on the alloy particles is still visible.

The SEM and XRD results show that alloy/graphite/PVDF(600 °C) coating is likely a composite of the active particles with a small amount of carbon residue. This is consistent with the findings of Hassan et al.[15] However, no particles could be found that showed

Fig. 4. SEM images of alloy/graphite/binder coatings cured at different temperatures: (*a*) alloy/graphite/PVDF(120 °C), (*b*) alloy/graphite/PVDF(600 °C), (*c*) alloy/graphite/PI(300 °C), and (*d*) alloy/graphite/PI(600 °C). Arrows in (*c*) and (*d*) indicate alloy surfaces coated with a rough layer of (*c*) PI or (*d*) carbonized (PI).

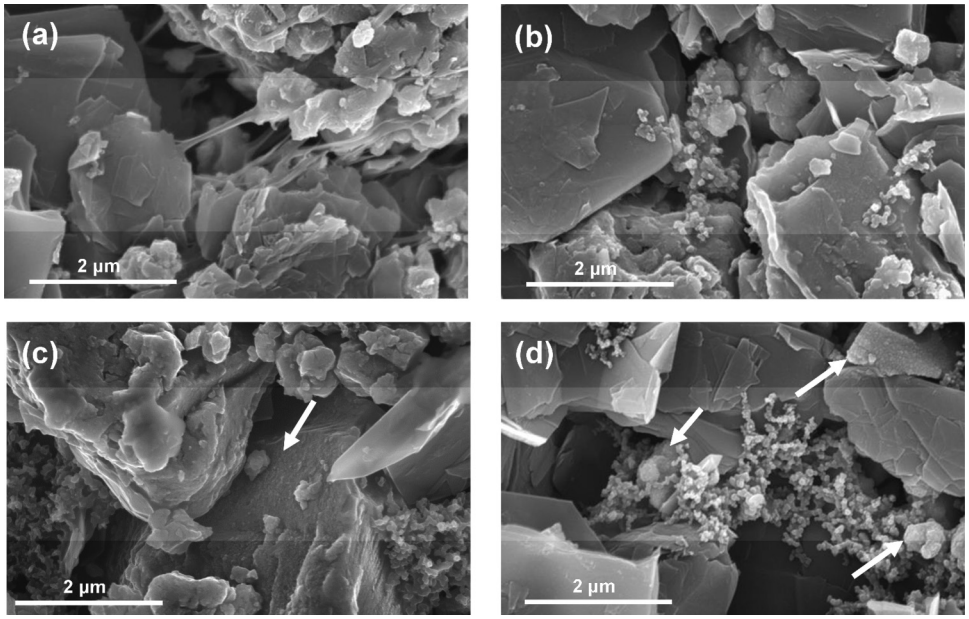

Fig. 5. (*a*) Potential vs. capacity and (*b*) cycling performance of an alloy/graphite/PVDF(120 °C) electrode; (*c*) potential vs. capacity and (*d*) cycling performance of an alloy/graphite/PVDF(600 °C) electrode. These electrodes were all formulated to have 10 wt% PVDF prior to heating. Also shown in blue in Fig. 5*d* is the cycling performance of an alloy/graphite/PVDF(600 °C) electrode having 20 wt% PVDF prior to heating. [Colour online.]

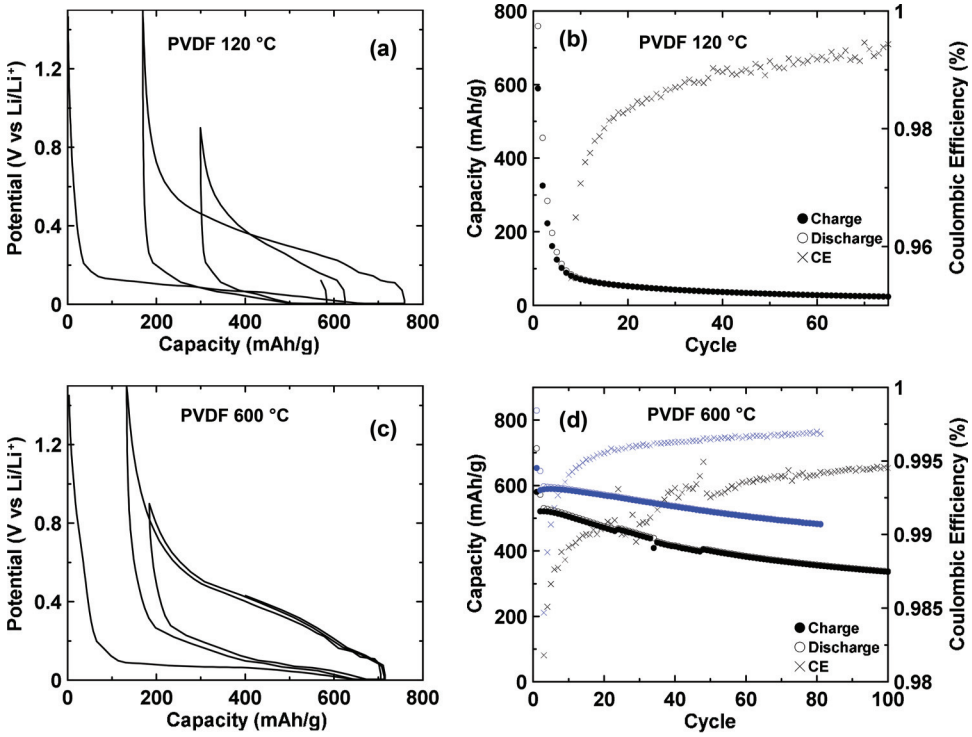

any sign of carbon coating. This is likely because of the small amount of carbon residue in the alloy/graphite/PVDF(600 °C) due to PVDF's large mass loss during heating, as indicated by TGA. In contrast, the alloy/graphite/PI(600 °C) coating comprises composite of active particles with a much greater carbon content. The amount of carbon is sufficient to uniformly coat all of the alloy particles in the coating, as observed by SEM.

Figure 5*a* shows the potential versus capacity plot of an alloy/graphite/PVDF(120 °C) electrode. We have reported good cycling for the same electrode formulation using PI, Phenolic Resin, and LiPAA binders in previous studies.[9,10,19] The first discharge of the alloy/graphite/PVDF(120 °C) electrode is comparable with that shown in Du et al.[19] using LiPAA binder. However, the irreversible capacity is significantly higher, and even though only 2.5 cycles

Fig. 6. (*a*) Potential vs. capacity and (*b*) cycling performance of an alloy/graphite/PI(300 °C) electrode; (*c*) potential vs. capacity and (*d*) cycling performance of an alloy/graphite/PI(600 °C) electrode.

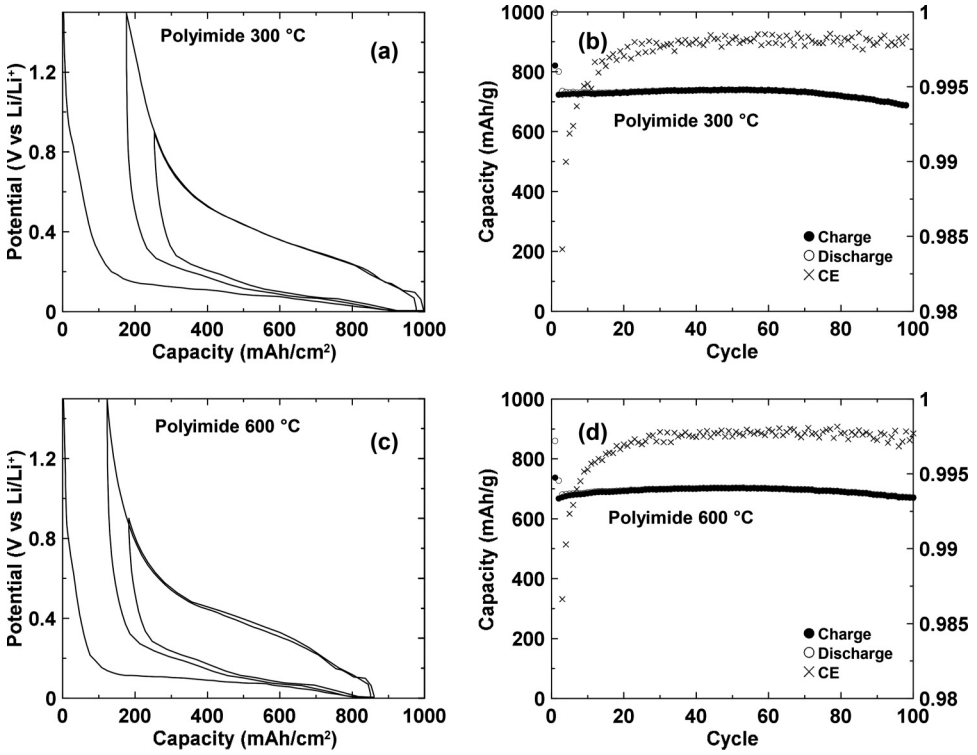

are shown, there are clear signs of rapid capacity fade. Figure 5*b* shows the cycling performance of this cell and confirms that the cycle life is very poor, with little capacity remaining after only 10 cycles. This demonstrates the poor performance of alloy electrodes with PVDF binder, which is well known.[1] This poor performance is likely due to the observed morphology of PVDF (Fig. 4*a*), which forms filaments in the coating rather than forming a uniform coating on the particles.[1]

Figure 5*c* shows the potential versus capacity curve for an alloy/graphite/PVDF(600 °C) electrode. The first cycle potential vs. capacity curve of this cell is similar to that of the cell in Fig. 5*a*; however, there is additional capacity at the beginning of the first discharge above 0.2 V. This is consistent with the additional capacity observed when a TiN/PVDF electrode was heated to 600 °C, as shown in Fig. 3*c*. Despite this additional initial capacity, the total first cycle discharge capacity of the alloy electrode heated at 600 °C is less than that of the electrode heated at 120 °C. We ascribe these effects to changes in the alloy structure, which results in capacity reduction upon heating to 600 °C due to grain growth. The cycling performance of the alloy/graphite/PVDF(600 °C) electrode, shown in Fig. 5*d*, is much improved over the alloy/graphite/PVDF(120 °C) electrode, shown in Fig. 5*b*. This is consistent with the findings of Hassan et al., who attribute this effect to the formation of a conductive carbon coating on the active particles.[15] Here, no such coating was observed and the electrode still has significant capacity fade, retaining only about 65% of its initial reversible capacity after 100 cycles and poor coulombic efficiencies of less than 99.5%.

Figure 6*a* shows the potential versus capacity curve for an alloy/graphite/PI(300 °C) electrode. The first discharge potential vs. capacity curve of this electrode also has significant capacity above 0.2 V, which we ascribe to the reduction of PI binder, as previously reported.[9] This is also consistent with the large first cycle PI reduction capacity shown in Fig. 3*d*. As we have reported previously,[9] this electrode has excellent cycle life, retaining about 95% of its initial capacity after 100 cycles and good coulombic efficiencies that exceed 99.8% after cycle 40, as shown in Fig. 6*b*. This good cycling performance was attributed to the formation of conductive carbon produced by the reduction of PI during the first cycle.[9] Figure 6*c* shows the potential versus capacity curve of an alloy/graphite/PI(600 °C) electrode. Additional capacity above 0.2 V, compared with an alloy/graphite/PVDF(120 °C) electrode, is also present during the first discharge, which is consistent with the significant first discharge capacity of PI heated to 600 °C, as shown in Fig. 3*e*. The alloy/graphite/PI(600 °C) electrode has about 20 mAh g^{-1} less reversible capacity than the same electrode heated to 300 °C, shown in Fig. 6*a*, again because of the lowered alloy capacity at 600 °C, as discussed above. Figure 6*d* shows the cycling performance of the alloy/graphite/PI(600 °C) electrode. The cycling performance is excellent with almost no capacity loss in 100 cycles. This is a significant improvement in the cycling performance compared with the same electrode cured at 300 °C, which lost 5% capacity in the same number of cycles.

The difference in cycling performance of the alloy/graphite electrode using PVDF binder heated to 600 °C in Ar, shown in Fig. 5*d*, compared with the electrode made under the same conditions except with PI binder, shown in Fig. 6*d*, is striking. The alloy/graphite/PI(600 °C) electrode performs much better than the alloy/graphite/PVDF(600 °C) electrode. One reason for this performance might be related to the difference in mass loss that results when PVDF and PI are heated, as shown in Fig. 1. During carbonization at 600 °C, PVDF loses considerably more mass than PI. Therefore, very little residual carbon remains when a PVDF electrode is heated to this temperature compared with a PI electrode with the same formulation. As mentioned above, the additional carbon in the heated PI electrode can uniformly coat the active particles. This may inhibit electrolyte decomposition reactions and improve cycling.

To see if the lack of residual carbon is the cause of the poor performance of the PVDF electrode, an alloy/graphite/PVDF(600 °C) electrode was prepared with double PVDF content, to compensate for its additional weight loss during heating, compared with PI.

Fig. 7. SEM image of an alloy/graphite/PVDF(600 °C) electrode having 20 wt% PVDF prior to heating. The arrow in the figure indicates an alloy surface coated with a rough layer of carbonized PVDF.

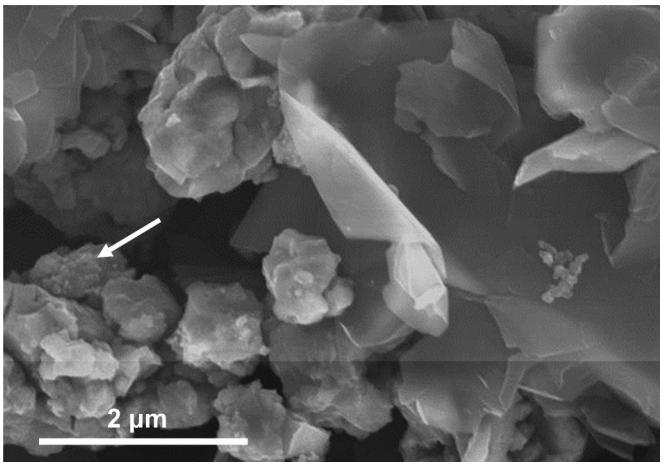

An SEM image of this coating is shown in Fig. 7. Some of the alloy is now coated with carbon in this electrode. Therefore, the increased amount of PVDF has resulted in some of the alloy surfaces becoming carbon coated after heating. However, the coating is not complete, as in the case of PI, and some of the alloy surfaces still appear pristine. The cycling performance of this electrode is shown in Fig. 5*d*. Increasing the PVDF content does result in significant improvements in cycle life and coulombic efficiency. However, the cycling performance of the alloy/graphite/PVDF(600 °C) electrode with excess PVDF is still inferior to the alloy/graphite/PI(600 °C) electrode. This is likely due to PI's ability to uniformly coat the active material particles, which leads to a uniform carbon coating upon heating. Even when the PVDF content is doubled, an insufficient amount of carbon residue is present to completely coat the alloy particles.

From these results, we speculate that the improved cycling due to carbonizing alloy electrodes is from the formation of a carbon coating on the alloy particles. The cycling is optimized when the carbon coating uniformly coats the alloy particles, leaving no bare alloy surfaces in contact with electrolyte. Based on these conclusions, carbon precursors such as PI that have a high carbon yield upon heating are ideal for forming carbonized alloy electrodes with good cycling performance, because they are more likely to form a uniform carbon coating on the alloy particles, compared with low carbon yield polymers such as PVDF.

Conclusion

It was found that heat treating electrode coatings with PI or PVDF binders to 600 °C in an inert atmosphere greatly improves their charge discharge cycling performance. During this heat treatment, these polymers decompose and carbonize. The cycle life of cells made using electrodes with PVDF binder that were heated at 600 °C have greatly superior cycle life compared with PVDF electrodes heated at temperatures below its carbonization temperature. Even better cycling performance is obtained for Si alloy electrodes with PI binder that were heated to 600 °C. The cycling performance of the Si alloy electrodes with PI binder cells heated to 600 °C was also superior to Si alloy electrodes with PI binder that were heated to 300 °C, and the irreversible capacity was slightly reduced. The observation that binders work well after thermal carbonization is further evidence that good binders such as PI become electrochemically reduced to form hydrogen-containing carbons.

It was speculated here that the superior performance of sintered PI binder compared with sintered PVDF binder is due to PI's higher carbon yield during thermal decomposition. As a result of this high carbon yield, a uniform carbon coating on the alloy particles could be attained with PI binders after carbonizing the electrode. This suggests that carbonizing aromatic carbons (soft carbon precursors) with high carbon yield may result in binders for alloy electrodes with good cycling properties. We have confirmed that this is true for sintered phenolic resin electrodes, which have a similar carbon yield as PI and a similar cycling performance. We plan to report on the relation of carbon yield and cycling performance in a future publication.

Acknowledgements

The authors acknowledge funding from NSERC and 3M Canada under the auspices of the Industrial Research Chair and Discovery grant programs. We also acknowledge the support of the Canada Foundation for Innovation, the Atlantic Innovation Fund and other partners that fund the Facilities for Materials Characterization managed by the Institute for Research in Materials at Dalhousie University.

References

(1) Obrovac, M. N.; Chevrier, V. L. *Chem. Rev.* **2014**, *114*, 11444. doi:10.1021/cr500207g.
(2) Obrovac, M. N.; Christensen, L. *Electrochem. Solid-State Lett.* **2004**, *7*, A93. doi:10.1149/1.1652421.
(3) Obrovac, M. N.; Christensen, L.; Le, D. B.; Dahn, J. R. *J. Electrochem. Soc.* **2007**, *154*, A849. doi:10.1149/1.2752985.
(4) Li, J.; Christensen, L.; Obrovac, M. N.; Hewitt, K. C.; Dahn, J. R. *J. Electrochem. Soc.* **2008**, *155*, A234. doi:10.1149/1.2830545.
(5) Hochgatterer, N. S.; Schweiger, M. R.; Koller, S.; Raimann, P. R.; Wöhrle, T.; Wurm, C.; Winter, M. *Electrochem. Solid-State Lett.* **2008**, *11*, A76. doi:10.1149/1.2888173.
(6) Bridel, J.-S.; Azaïs, T.; Morcrette, M.; Tarascon, J.-M.; Larcher, D. *J. Electrochem. Soc.* **2011**, *158*, A750. doi:10.1149/1.3581024.
(7) Komaba, S.; Yabuuchi, N.; Ozeki, T.; Han, Z.; Shimomura, K.; Yui, H.; Katayama, Y.; Miura, T. *J. Phys. Chem. C* **2012**, *116*, 1380. doi:10.1021/jp204817h.
(8) Komaba, S.; Shimomura, K.; Yabuuchi, N.; Ozeki, T.; Yui, H.; Konno, K. *J. Phys. Chem. C* **2011**, *115*, 13487. doi:10.1021/jp201691g.
(9) Wilkes, B. N.; Brown, Z. L.; Krause, L. J.; Triemert, M.; Obrovac, M. N. *J. Electrochem. Soc.* **2016**, *163*, A364. doi:10.1149/2.0061603jes.
(10) Hatchard, T. D.; Bissonnette, P.; Obrovac, M. N. *J. Electrochem. Soc.* **2016**, *163*, A2035. doi:10.1149/2.1121609jes.
(11) Wang, C.; Wu, H.; Chen, Z.; McDowell, M. T.; Cui, Y.; Bao, Z. *Nat. Chem.* **2013**, *5*, 1042. doi:10.1038/nchem.1802.
(12) Xun, S.; Song, X.; Battaglia, V.; Liu, G. *J. Electrochem. Soc.* **2013**, *160*, A849. doi:10.1149/2.087306jes.
(13) Wu, H.; Yu, G.; Pan, L.; Liu, N.; McDowell, M. T.; Bao, Z.; Cui, Y. *Nat. Commun.* **2013**, *4*, 1943. doi:10.1038/ncomms2941.
(14) Yoon, T.; Chapman, N.; Nguyen, C. C.; Lucht, B. L. *J. Mater. Sci.* **2017**, *52*, 3613. doi:10.1007/s10853-016-0442-2.
(15) Hassan, F. M.; Chabot, V.; Elsayed, A. R.; Xiao, X.; Chen, Z. *Nano Lett.* **2014**, *14*, 277. doi:10.1021/nl403943g.
(16) Zheng, T.; Liu, Y.; Fuller, E. W.; Tseng, S.; von Sacken, U.; Dahn, J. R. *J. Electrochem. Soc.* **1995**, *142*, 2581. doi:10.1149/1.2050057.
(17) Grugeon, S.; Laruelle, S.; Herrera-Urbina, R.; Dupont, L.; Poizot, P.; Tarascon, J.-M. *J. Electrochem. Soc.* **2001**, *148*, A285. doi:10.1149/1.1353566.
(18) Zheng, T.; McKinnon, W. R.; Dahn, J. R. *J. Electrochem. Soc.* **1996**, *143*, 2137. doi:10.1149/1.1836972.
(19) Du, Z.; Dunlap, R. A.; Obrovac, M. N. *J. Electrochem. Soc.* **2014**, *161*, A1698. doi:10.1149/2.0941410jes.